Single-Molecule-Resolved Structural Changes Induced by Temperature and Light in Surface-Bound Organometallic Molecules Designed for Energy Storage

Jongweon Cho,[†,‡,#,*] Luis Berbil-Bautista,[†,§] Ivan V. Pechenezhskiy,[†,‡] Niv Levy,[†,§,△] Steven K. Meier,[⊥] Varadharajan Srinivasan,[∥,▼] Yosuke Kanai,[¶] Jeffrey C. Grossman,[∥] K. Peter C. Vollhardt,[⊥] and Michael F. Crommie[†,‡,§,*]

[†]Department of Physics, and [‡]Center of Integrated Nanomechanical Systems, University of California at Berkeley, Berkeley, California 94720, United States, [§]Materials Sciences Division, Lawrence Berkeley National Laboratory, Berkeley, California 94720, United States, [⊥]Department of Chemistry, University of California at Berkeley, Berkeley, California 94720, United States, [∥]Department of Materials Science and Engineering, Massachusetts Institute of Technology, Cambridge, Massachusetts 02139, United States, and [¶]Condensed Matter and Materials Division, Lawrence Livermore National Laboratory, Livermore, California 94554, United States. [#] Present address: Center for Nanoscale Materials, Argonne National Laboratory, Argonne, Illinois 60439. [△] Present address: Center for Nanoscale Science and Technology, National Institute of Standards and Technology, Gaithersburg, Maryland 20899. [▼] Present address: Department of Chemistry, Indian Institute of Science Education and Research Bhopal, ITI (Gas Rahat) Building, Govindpura, Bhopal 426023, Madhya Pradesh, India.

ABSTRACT We have used scanning tunneling microscopy, Auger electron spectroscopy, and density functional theory calculations to investigate thermal and photoinduced structural transitions in (fulvalene)tetracarbonyldiruthenium molecules (designed for light energy storage) on a Au(111) surface. We find that both the parent complex and the photoisomer exhibit striking thermally induced structural phase changes on Au(111), which we attribute to the loss of carbonyl ligands from the organometallic molecules. Density functional theory calculations support this conclusion. We observe that UV exposure leads to pronounced structural change only in the parent complex, indicative of a photoisomerization reaction.

KEYWORDS: scanning tunneling microscopy · fulvalene · ruthenium · CO loss · isomerization · energy storage

Discovery of new materials systems capable of efficiently converting and storing solar energy is an urgent challenge mandated to address growing global energy needs.[1] Photo- and thermally isomerizable organometallic molecules have many positive attributes for this application due to their generally favorable optical absorption properties and their chemically tunable structures which allow for optimization of energy efficiency.[2,3] A robust system known to have the capacity to store solar energy is (fulvalene)tetracarbonyldiruthenium [$FvRu_2(CO)_4$].[4] This molecule converts photonic energy to chemical energy through photoisomerization, that is, the optically induced conformational change of the molecule to a high-energy isomer form (Figure 1). The stored chemical energy (enthalpy difference of ~0.9 eV) is highly stable (experimentally measured barrier for thermal reversal reaction of ~1.3 eV)[5] and can be extracted in a straightforward manner by mild heating.[4] Potential future applications of such molecules for energy use require understanding and controlling their behavior in new environments, including in the presence of nearby surfaces. While this molecule has been studied for more than a decade,[4−9] its behavior at a surface is not understood. Understanding the interactions of the molecules with surfaces is of critical importance for further tailoring their surface-catalytic behavior in view of potential photochemical energy storage devices. Scanned probe microscopy is a particularly useful technique for exploring the local behavior of such organometallic species at surfaces.[10,11]

We have used variable-temperature ultrahigh vacuum (UHV) scanning tunneling microscopy (STM), Auger electron spectroscopy (AES), and density functional theory (DFT) calculations to investigate thermal and photoinduced structural transitions in $FvRu_2(CO)_4$ molecules on Au(111) at the single-molecule level. We find that both the parent complex and the photoisomer exhibit new temperature-dependent structural phases at a surface. We propose that thermally induced CO loss takes place for both the parent complex and the photoisomer adsorbed onto Au(111), based on STM topographic images and DFT calculations.

* Address correspondence to crommie@berkeley.edu, jwcho@anl.gov.

Received for review January 4, 2011 and accepted April 11, 2011.

Published online April 11, 2011
10.1021/nn2000367

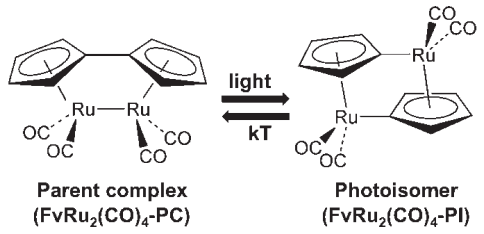

Figure 1. Schematic diagram showing photoisomerization and thermal reversal of $FvRu_2(CO)_4$.

UV exposure results in photoinduced structural changes only for the parent complex, suggesting that the parent complex photoisomerizes at the surface of Au(111).

RESULTS

We observe that when the parent complex [$FvRu_2(CO)_4$-PC] is deposited onto Au(111) in submonolayer amounts it self-assembles into two-dimensional molecular islands in the low-temperature phase (phase 1), as shown in Figure 2a. Single molecules are identified by the repeated unit cell seen in STM topographic images and outlined by a white border in the inset. They appear as a pair of symmetric lobes that have an overall length approximately matching the expected length of a $FvRu_2(CO)_4$ molecule.

These patterns change when the molecule-decorated surface is subjected to extended annealing at room temperature, as seen in Figure 2b. The two-dimensional molecular islands disappear, and a new structural phase (the high-temperature phase, or phase 2) emerges. Individual molecules in phase 2 appear as a pair of asymmetric lobes, as outlined in the white border in the inset (they display a bent "lima bean" shape). The molecules in phase 2 closely follow the underlying Au(111) herringbone surface reconstruction.[12] The two observed structural phases of the parent complex (phases 1 and 2) are homogeneous throughout the sample, and we do not observe the two phases simultaneously.

In order to gain further insight into isomer-dependent surface behavior of $FvRu_2(CO)_4$, we examined its photoisomer [$FvRu_2(CO)_4$-PI] adsorbed onto Au(111) under the same conditions as the parent complex. We find that the photoisomer also self-assembles into two-dimensional molecular islands when it is in the low-temperature phase (phase 1*), as shown in Figure 3a. These appear slightly less corrugated than phase 1 islands of the parent complex, and the intermolecular packing does not appear to be completely uniform within the islands, making it difficult to identify the structure of individual phase 1* molecules. STM manipulation techniques were utilized[13] to attempt detachment of individual molecules from an island, but these attempts (not shown) typically resulted in the lateral displacement of whole molecular islands (up to 7×7 nm^2) by tens of nanometers, indicating that

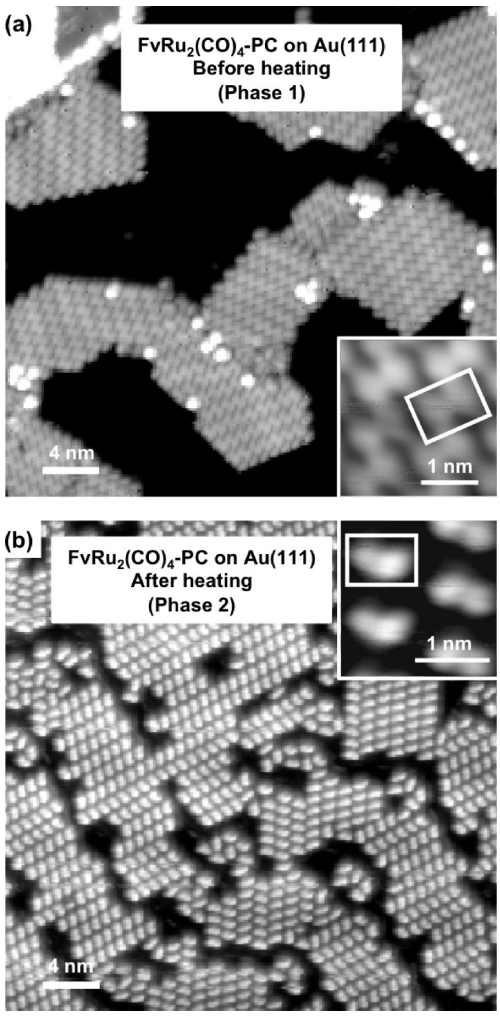

Figure 2. Low-temperature (12 K) STM topographic images of $FvRu_2(CO)_4$ parent complex adsorbed onto a Au(111) surface (a) before (phase 1) and (b) after (phase 2) extended annealing at room temperature (imaging parameters $V = +1$ V (sample bias), $I = 50$ pA). Insets show close-up views of phase 1 and phase 2 molecular morphologies; individual molecules are outlined with white borders.

molecule−molecule interactions in phase 1* are greater than molecule−surface interactions.

When phase 1* of the photoisomer is annealed longer at room temperature, the molecules dramatically change their conformation and develop into a new high-temperature phase (phase 2*), as shown in Figure 3b. This new phase 2* of the photoisomer is similar to phase 2 of the parent complex in that the individual molecules become more isolated and closely follow the underlying Au(111) surface reconstruction. The phase 2* molecules, however, have a very different symmetry compared to the phase 2 molecules of the parent complex (they have a more symmetrical oval shape rather than a bent lima bean shape).

To characterize the stoichiometric composition of $FvRu_2(CO)_4$/Au(111), we performed AES on a Au(111) surface decorated with the parent complex in phase 1, which was first imaged at low temperature with the

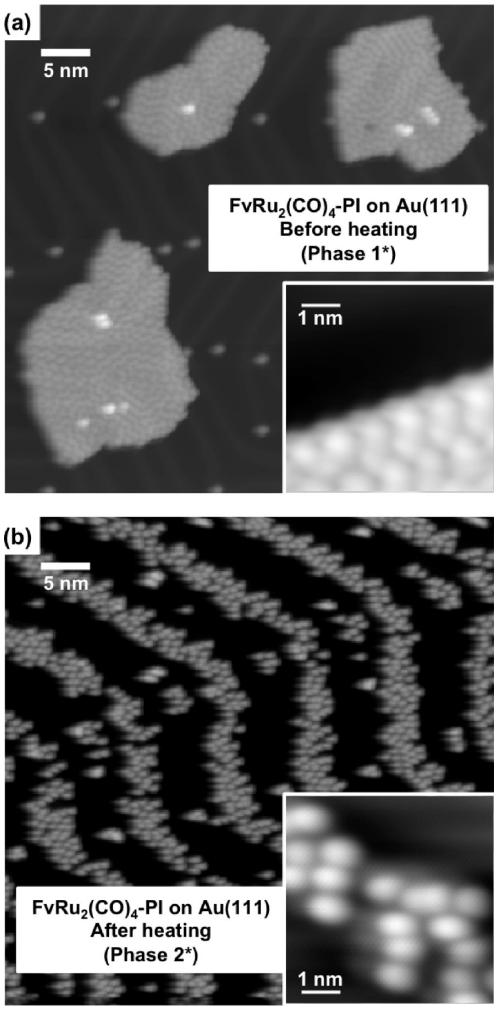

Figure 3. Low-temperature (12 K) STM topographic images of $FvRu_2(CO)_4$-PI adsorbed onto a Au(111) surface (a) before (phase 1*) and (b) after (phase 2*) extended annealing at room temperature (imaging parameters $V = +1$ V (sample bias), $I = 50$ pA). Insets show close-up views of phase 1* and phase 2* molecular morphologies.

STM (to verify the phase) and which was then warmed to room temperature for AES measurements. Multiple AES measurements were performed at room temperature over a period of time ranging from 10 min to several hours after removing the sample from the low-temperature STM stage. These measurements were compared to AES measurements of a bare Au(111) surface, also held at room temperature. We find that the parent-complex-decorated gold surface exhibits a strong enhancement of carbon and ruthenium (as measured by AES) compared to bare gold but shows only minimal enhancement of the oxygen AES signal compared to bare gold. The AES measurements of the molecule-decorated Au sample showed no time dependence over the range of times described above. The estimated ratios of Ru/C/O extracted from the AES spectra[14] are consistent with a loss of roughly 90% of the carbonyl groups from the adsorbed molecular layer. It is unclear from the Auger measurements alone, however, whether this loss arises from thermal annealing effects or from excitation/damage due to the electron beam of the Auger spectrometer.

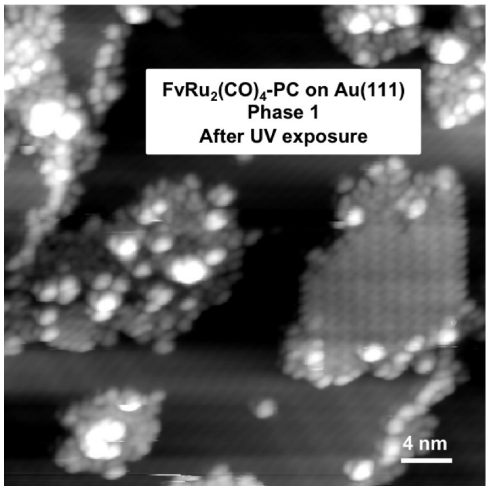

Figure 4. Low-temperature (12 K) STM topographic image of $FvRu_2(CO)_4$ parent complex (phase 1) on Au(111) after 12 h of UV light exposure ($\lambda = 375$ nm) at low temperature ($12\ K < T < 15\ K$). Photoinduced structural disorder can be seen.

We additionally explored photoisomerization of $FvRu_2(CO)_4$ on gold by illuminating each structural phase of both the parent complex and the photoisomer with UV light. We find that only phase 1 of the parent complex exhibits a photoinduced structural change, while the other three phases remain completely unchanged. Figure 4 shows the structural change observed in phase 1 of the parent complex after 12 h of UV (375 nm) exposure at low temperature ($12\ K < T < 15\ K$) [this should be compared to the pristine phase 1]. Pronounced regions of disorder are seen to emerge within phase 1 molecular islands. We observe that the degree of disorder in phase 1 molecular islands monotonically increases as UV exposure is increased.

DISCUSSION

Thermally Induced Structural Change: CO Loss. We first discuss our experimental observation of irreversible structural change in the $FvRu_2(CO)_4$ parent complex as it switches from phase 1 to phase 2 in response to thermal annealing at room temperature. The most straightforward explanation for this behavior is that the parent complex loses its carbonyl groups upon extended room temperature annealing. This mechanism is consistent with the AES data, but interpretation of the AES data is complicated by the possibility of electron-beam-induced damage, and so we rely more heavily here on STM data that were taken on samples not subjected to Auger electron spectroscopy. The STM data, in combination with our DFT calculations, support the thermally induced carbonyl loss mechanism. This can be seen first by the observed competition between molecule–molecule interactions *versus* molecule–surface interactions in phase 1 and phase 2 of the parent

complex. In the low-temperature phase (phase 1), the Au(111) surface reconstruction is visible through the molecular islands and appears unperturbed, suggesting a weak molecule–surface interaction for phase 1. In the high-temperature phase (phase 2), however, the molecules appear separate from each other and follow the underlying surface reconstruction, indicating a stronger molecule–surface interaction for phase 2 molecules. This is consistent with CO removal from the molecules as they transition from phase 1 to phase 2, as this would expose the Ru atoms of the parent complex and facilitate a stronger interaction between the molecule and surface due to metallic bonding between Ru and Au.[15] This idea is also consistent with DFT calculations that we performed to investigate stable adsorption configurations of $FvRu_2(CO)_4$ parent complex on Au(111). We considered three configurations in our calculations: (i) the upright molecule with the Ru atoms pointing toward the Au surface, (ii) the flipped molecule with the Fv ring on the surface, and (iii) a side-ways configuration with the two Ru atoms as well as H atoms from the Fv ring pointing toward the surface (see Supporting Information). Our calculations indicate that the $FvRu_2(CO)_4$ parent complex preferentially lies with its Fv ring on the surface [configuration (ii); Figure 5a] but then becomes tilted in a side-ways configuration [configuration (iii); Figure 5b] when its carbonyl groups are removed. The adsorption energy also increases from 0.11 to 0.46 eV once the carbonyl groups are dissociated from the molecule, consistent with the interpretation that the surface–molecule interaction is enhanced without the carbonyl groups. We note that the parent complex $FvRu_2$ fragments (without the carbonyl groups) have precisely the same symmetry as the lima bean shaped molecules observed in phase 2.

We believe that the photoisomer of $FvRu_2(CO)_4$ undergoes a similar loss of CO groups as it transitions from phase 1* to phase 2* upon room temperature annealing. This is consistent with the fact that the CO-Ru bond strength is similar for both the $FvRu_2(CO)_4$ parent complex and the photoisomer.[4] In addition, the self-assembly behavior seen for both phase 1* and phase 2* (photoisomer molecules) is extremely similar to the self-assembly behavior seen for phase 1 and phase 2 (parent complex molecules), respectively. This implies a similar competition between molecule–molecule and molecule–surface interactions for both the parent complex and the photoisomer, and thus a similar transition mechanism between low-temperature and high-temperature phases. The thermally induced CO loss is also consistent with our observation that phase 2* monomers of the photoisomer exhibit a different morphological symmetry compared to phase 2 monomers since, for phase 2* monomers, we expect the Ru atoms to lie diagonally across the $FvRu_2$ fragment, as can be seen in Figure 1 (photoisomer without CO groups).

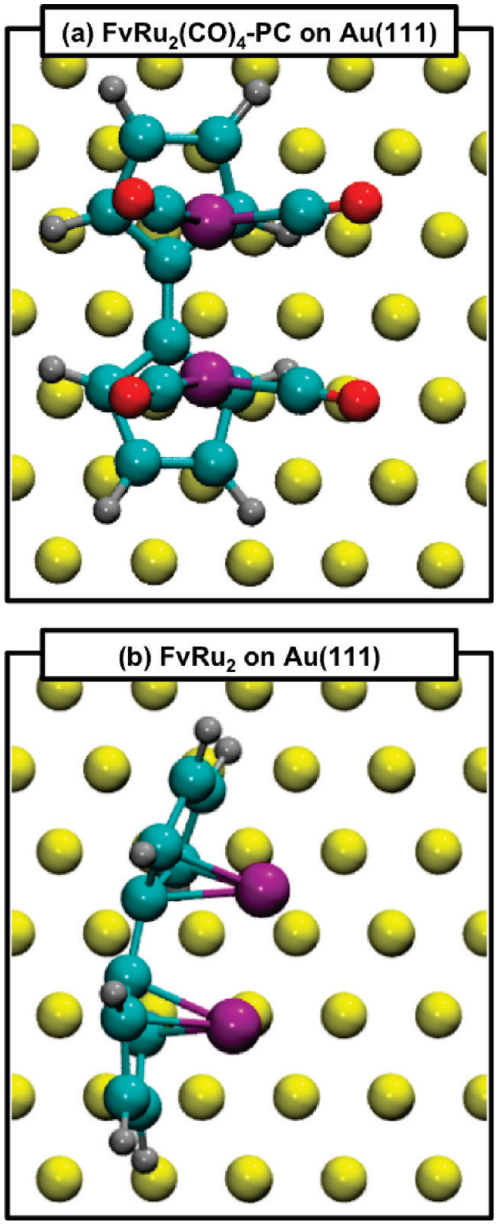

Figure 5. Results of DFT calculations show relaxed adsorption geometry of the parent complex on Au(111): (a) with CO groups and (b) without CO groups (*i.e.*, $FvRu_2$ fragment). Gold, carbon, ruthenium, oxygen, and hydrogen atoms are indicated by yellow, cyan, purple, red, and gray, respectively.

Light-Induced Structural Change: Photoisomerization. We now discuss our observation that UV exposure causes structural transformation only in phase 1 of the parent complex on Au(111). We believe that the emergent structural disorder seen after UV exposure in phase 1 (Figure 4) is indicative of photoisomerization of the parent complex to phase 1* of the photoisomer, although it is difficult to directly verify in our measurements due to (i) the disordered appearance of the height change seen in STM images and (ii) possible transitions to multiple metastable structural configurations, as suggested by a recent work.[5] Photoisomerization of the parent complex

is consistent with the fact that dinuclear single metal−metal bonded carbonyls are known to undergo metal−metal bond cleavage upon UV exposure.[2] We also expect a significantly higher probability of photoisomerization in the parent complex (phase 1) (which is known to photoisomerize in solution) compared to the probability of photoisomerization in the already photoisomerized complex (phase 1*) and the $FvRu_2$ fragments (phase 2 and phase 2*). The observed low yield of the photoinduced structural change in phase 1 suggests a low photoswitching efficiency for this molecule at a metallic surface compared to the switching efficiency seen when this molecule is in solution.[16] It is possible that the presence of the Au surface reshapes the molecular potential energy landscape, thus changing the photoisomerization dynamics of surface-bound organometallic molecules.[17]

CONCLUSIONS

We have investigated the self-assembly and photoswitching properties of both the parent complex and the photoisomer of $FvRu_2(CO)_4$ molecules adsorbed onto Au(111) in the submonolayer regime. Thermally induced CO loss for both the parent complex and the photoisomer is proposed based on our STM, AES, and DFT results. UV-induced disorder is observed in the low-temperature phase of the parent complex and is attributed to the photoisomerization of this complex on Au(111). The presence of a metallic surface is seen to strongly influence the thermal and photoinduced behavior of $FvRu_2(CO)_4$.

METHODS

Our measurements were performed using a home-built variable-temperature UHV STM. A clean Au(111) substrate was prepared by repeated cycles of argon-ion sputtering and annealing. The synthesis of $FvRu_2(CO)_4$ is described in ref 6 and synthesis of the photoisomer in ref 4. Both the parent complex and the photoisomeric form of $FvRu_2(CO)_4$ were deposited *via* thermal evaporation onto clean Au(111) substrates held at 12 K (see Supporting Information). For the low-temperature phase, the sample was removed from the cryogenic STM stage using a room temperature manipulator and held for 10 min before subsequent measurements. During this 10 min interval, we estimate (based on thermal time constants) that the temperature of the sample rises from 12 K to 260 ± 30 K. For the high-temperature phase, the sample was held at room temperature for more than 1.5 h, during which time it was in thermal equilibrium with the surrounding environment. Tunnel currents were kept below 55 pA to prevent interaction between the STM tip and the molecules. AES measurements were conducted using an Omicron CMA detector in UHV. The electron beam energy and the beam current were 3 keV and 1.5 μA, respectively. A cw diode laser aligned at an external viewport provided UV (375 nm) radiation at the sample surface with average intensity of 92 mW/cm^2. During laser exposure, the STM tip was retracted from the surface and the sample temperature was maintained between 12 and 15 K. DFT calculations were performed to investigate energetically preferred configurations for the parent complex on Au(111), with PBE approximations to the exchange-correlation effects.[18−22]

Acknowledgment. STM instrumentation development and measurements supported by the Director, Office of Science, Office of Basic Energy Sciences, Division of Materials Sciences and Engineering Division, U.S. Department of Energy under Contract No. DE-AC03-76SF0098; STM data analysis supported by the National Science Foundation within the Center of Integrated Nanomechanical Systems, under Grant EEC-0425941; molecular synthesis supported by the Sustainable Products and Solutions Program at UC Berkeley and the NSF (CHE-0907800); numerical simulations supported by the U.S. Department of Energy at Lawrence Livermore National Laboratory under Contract DE-AC52-07NA27344.

Supporting Information Available: Computational details, scheme of the molecular configurations investigated by DFT calculations, Cartesian coordinates of the molecular configurations shown in Figure 5, and description of NMR experiments to confirm the capability of thermal sublimation of the photoisomer with <4% thermal conversion to the parent complex. This material is available free of charge *via* the Internet at http://pubs.acs.org.

REFERENCES AND NOTES

1. Crabtree, G. W.; Lewis, N. S. Solar Energy Conversion. *Phys. Today* **2007,** *60*, 37–42.
2. Geoffroy, G. L.; Wrighton, M. S. Organometallic Photochemistry. In *Organometallic Photochemistry*; Academic Press: New York, 1979.
3. Wang, M. S.; Xu, G.; Zhang, Z. J.; Guo, G. C. Inorganic−Organic Hybrid Photochromic Materials. *Chem. Commun.* **2010,** *46*, 361–376.
4. Boese, R.; Cammack, J. K.; Matzger, A. J.; Pflug, K.; Tolman, W. B.; Vollhardt, K. P. C.; Weidman, T. W. Photochemistry of (Fulvalene)Tetracarbonyldiruthenium and Its Derivatives: Efficient Light Energy Storage Devices. *J. Am. Chem. Soc.* **1997,** *119*, 6757–6773.
5. Kanai, Y.; Srinivasan, V.; Meier, S. K.; Vollhardt, K. P. C.; Grossman, J. C. Mechanism of Thermal Reversal of the (Fulvalene)Tetracarbonyldiruthenium Photoisomerization: Toward Molecular Solar-Thermal Energy Storage. *Angew. Chem., Int. Ed.* **2010,** *49*, 8926–8929.
6. Vollhardt, K. P. C.; Weidman, T. W. Synthesis, Structure, and Photochemistry of Tetracarbony(fulvalene)diruthenium—Thermally Reversible Photoisomerization Involving Carbon−Carbon Bond Activation at a Dimetal Center. *J. Am. Chem. Soc.* **1983,** *105*, 1676–1677.
7. Vollhardt, K. P. C.; Weidman, T. W. Efficient Syntheses of New Fulvalene-Bridged Carbonyl Complexes of Cobalt, Ruthenium, Chromium, Molybdenum, and Tungsten. *Organometallics* **1984,** *3*, 82–86.
8. Drage, J. S.; Tilset, M.; Vollhardt, P. C.; Weidman, T. W. First Photosubstitution Chemistry of Fulvalene-Bridged Metal−Metal Bonded Carbonyls: Synthesis and Structural Determination of Novel Homobimetallic and Heterobimetallic Alkyne Complexes. *Organometallics* **1984,** *3*, 812–814.
9. Boese, R.; Tolman, W. B.; Vollhardt, K. P. C. Carbonyl Substitution and Ring Slippage upon Reaction of Trialkylphosphines with (Fulvalene)diruthenium Tetracarbonyl. X-ray Structural Analysis of $(\eta^0{:}\eta^4\text{-}C_{10}H_8)Ru(PMe_3)_2CO$ and Fluxional Behavior of $(\eta^5{:}\eta^5\text{-}C_{10}H_8)Ru_2(CO)_3L$ (L = Phosphine). *Organometallics* **1986,** *5*, 582–584.
10. Braun, K. F.; Iancu, V.; Pertaya, N.; Rieder, K. H.; Hla, S. W. Decompositional Incommensurate Growth of Ferrocene Molecules on a Au(111) Surface. *Phys. Rev. Lett.* **2006,** *96*, 246102.
11. Yamachika, R.; Lu, X.; Wegner, D.; Wang, Y.; Wachowiak, A.; Grobis, M.; Beltran, L. M. C.; Long, J. R.; Pederson, M.; Crommie, M. F. Local Electronic Properties of Titanocene Chloride Dimer Molecules on a Metal Surface. *J. Phys. Chem. C* **2009,** *113*, 677–680.

12. Barth, J. V.; Brune, H.; Ertl, G.; Behm, R. J. Scanning Tunneling Microscopy Observations on the Reconstructed Au(111) Surface: Atomic Structure, Long-Range Superstructure, Rotational Domains, and Surface Defects. *Phys. Rev. B* **1990,** *42*, 9307.
13. Stroscio, J. A.; Eigler, D. M. Atomic and Molecular Manipulation with the Scanning Tunneling Microscope. *Science* **1991,** *254*, 1319–1326.
14. Davis, L. E.; MacDonald, N. C.; Palmberg, P. W.; Riach, G. E.; Weber, R. E. *Handbook of Auger Electron Spectroscopy*, 2nd ed.; Physical Electronics Industries, Inc.: Eden Prairie, MN, 1976.
15. Niemantsverdriet, J. W.; Dolle, P.; Markert, K.; Wandelt, K. Thermal-Desorption of Strained Monoatomic Ag and Au Layers from Ru(001). *J. Vac. Sci. Technol., A* **1987,** *5*, 875–878.
16. We consider photoswitching efficiency as the product of molecular optical absorption and quantum yield.
17. Comstock, M. J.; Strubbe, D. A.; Berbil-Bautista, L.; Levy, N.; Cho, J.; Poulsen, D.; Fréchet, J. M. J.; Louie, S. G.; Crommie, M. F. Determination of Photoswitching Dynamics through Chiral Mapping of Single Molecules Using a Scanning Tunneling Microscope. *Phys. Rev. Lett.* **2010,** *104*, 178301.
18. Giannozzi, P.; Baroni, S.; Bonini, N.; Calandra, M.; Car, R.; Cavazzoni, C.; Ceresoli, D.; Chiarotti, G. L.; Cococcioni, M.; Dabo, I.; *et al.* Quantum Espresso: A Modular and Open-Source Software Project for Quantum Simulations of Materials. *J. Phys.: Condens. Matter* **2009,** *21*, 395502.
19. Perdew, J. P.; Burke, K.; Ernzerhof, M. Generalized Gradient Approximation Made Simple. *Phys. Rev. Lett.* **1996,** *77*, 3865.
20. Ultrasoft pseudopotentials[21] were used to describe the valence−core interactions of electrons, including scalar relativistic effects of the core for Au and Ru atoms. Wave functions and charge densities were expanded in plane waves with kinetic energies up to 25 and 200 Ry, respectively. All geometries were relaxed until all forces on the atoms were less than 0.02 eV/Å. Marzari-Vanderbilt "cold smearing"[22] was used, together with Monkhorst-Pack k-point sampling of $3 \times 4 \times 1$ for Brillouin zone integration. The Au(111) surface was described by a 4-layer $\sqrt{3} \times 2$ slab with 16 atoms per layer (a coverage of 1 molecule in 119.18 Å^2 of the surface) with periodic boundary conditions. A vacuum of at least 15 Å was taken between the slabs in the surface normal direction.
21. Vanderbilt, D. Soft Self-Consistent Pseudopotentials in a Generalized Eigenvalue Formalism. *Phys. Rev. B* **1990,** *41*, 7892–7895.
22. Marzari, N. Ab-initio Molecular Dynamics for Metallic Systems. Ph.D. Dissertation, University of Cambridge, 1996.